



Effect of Gas Ratio on Tribological and Corrosion Properties of Ion Beam Sputter Deposited TiN Coatings

A. R. Grayeli Korpi^{*1}, P. Balashabadi¹, M. M. Larijani², M. Habibi³, A. Hamidi¹, M. Malek¹

¹ Physics and Accelerators Research School, Nuclear Science & Technology Research Institute (NSTRI), Box: 11365-3486, Tehran, Iran

² Radiation application Research School, Nuclear Science & Technology Research Institute (NSTRI), Box: 11365-3486, Tehran, Iran

³ Plasma Physics Research Center, Faculty of Sciences, Science and Research Branch, Islamic Azad University, P. O. Box: 14515/775, Tehran, Iran.

ARTICLE INFO

Article history:

Received: 6 May 2018

Final Revised: 30 Jun 2018

Accepted: 1 Jul 2018

Available online: 8 Jul 2018

Keywords:

TiN thin films

Corrosion

Potentiodynamic

Stainless steel

SEM

ABSTRACT

Titanium nitride thin films were grown on 304 stainless steel substrates at various nitrogen/argon flow ratios by ion beam sputtering (IBS) technique. The current research is a follow up study on the influence of gas ratio on structural and corrosion properties in the TiN coated 304 stainless steel. Film structural identification of phases was performed using X-ray diffractometry (XRD). Scanning electron microscope (SEM) was employed to study surface morphology and also elemental analysis of samples after corrosion test was conducted by energy dispersive spectroscopy (EDS). Through our results, we showed that the films deposited under an Ar: N₂ ratio of 50(sccm):7(sccm) exhibited a TiN(200) preferred orientation. The corrosion behavior of the samples was evaluated by potentiodynamic polarization test in 3.5% NaCl solution. A critical gas ratio was found at which the corrosion resistant was highest. The correlation between corrosion resistance, structural and surface morphology was examined. Prog. Color Colorants Coat. 11 (2018), 129-135 © Institute for Color Science and Technology.

1. Introduction

Transition-metal nitride thin films such as TiN and ZrN are a technologically important class of materials due to their mechanical properties as well as chemical stability. These materials are close-packed metallic structures in which nitrogen atoms occupy the interstitial sites. Bonding in this structure involves simultaneous contribution of covalent, ionic and metallic bonding to cohesive energy, which leads to very interesting properties [1, 2]. The triple bond

between Ti and N as well as the mixed p and d characteristics of the interaction between Ti 3d and N 2p represents an essential aspect of covalent bonding between titanium and nitrogen atoms. It is also responsible for its inert nature, mechanical hardness and high melting point [3]. It has been widely used to improve the performance and wear lifetime of cutting tools and drills [4, 5]. Development of Titanium nitride thin films technology has been one of the key efforts for the development of decorative purposes, due to

*Corresponding author: grayli@alumni.ut.ac.ir

their gold-like color [6]. TiN is also well known for its oxidation resistance property.

It is well known that tribological properties are not only intrinsic or inherent to specific materials, but are strongly dependent on system and process of production [7]. TiN thin films have been produced by various techniques, among them, physical vapor deposition (PVD) is an advanced vacuum coating technique, used widely for surface modification. Among the various subdivisions of PVD processes such as magnetron sputtering [8], pulsed laser ablation [9], and ion plating [10], ion beam deposition has been one of the most important and widely used techniques in recent decades to grow TiN thin films. It has been recognized that the most important parameters governing the physical properties of these films are the nitrogen partial pressure and deposition temperature [6].

Control of reactive sputtering processes, for the film stoichiometry, structure, and morphology are very important for the range of TiN_x applications, therefore several papers and methods on TiN, film deposition have already been published. The present work has been focused on deposition of TiN films on 304 stainless-steel substrates by ion beam technique using high-purity titanium (99.99%) target at 400 °C under various nitrogen/argon flow ratios. The ultimate goal is to implement the conditions under which TiN films can be prepared, and also to characterize the morphology and microstructural features of PVD TiN thin films.

2. Materials and Experimental Details

Austenitic AISI 304 stainless steel with the chemical composition shown in Table 1 was used in the experiments. The samples were cut from a same sheet with rectangular shapes of 20 mm × 20 mm.

TiN films were deposited on the stainless steel substrates by ion beam sputtering using high-purity titanium (99.99%) metallic plate target ($10 \times 10 \times 0.5 \text{ cm}^3$). The schematic diagram of the ion beam sputtering for deposition of TiN films is shown in Figure 1. The substrates were cleaned by rinsing in ultrasonic bath containing acetone and methanol and dried under nitrogen gas prior to loading into the deposition chamber.

The pressure control device consists of a penning gauge. The gases used are high-purity argon (99.999%) as the working gas and nitrogen (99.999%) as the reactive gas.

Before introducing the gases into the chamber, the coating chamber was evacuated by a two mechanical pumps and two diffusion pumps to a base pressure of 2.2×10^{-5} torr. The working pressure was maintained at 5.5×10^{-3} torr during film deposition, and the sputtering was carried out by introducing different Ar/N₂ gas ratios by keeping N₂ flux fixed at 7 sccm. Sputtering was performed at different Ar fluxes of 7, 15, 30 and 50 sccm. The substrate temperature during deposition was fixed at 400 °C. The detailed deposition conditions are summarized in Table 2.

Table 1: Chemical composition of AISI 304 stainless steel.

SS Type	Cr	Ni	Mn	Si	C
AISI 304	18.5	8.4	1.6	0.3	0.1

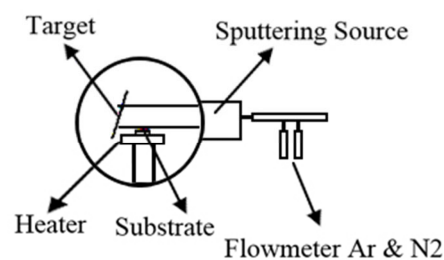


Figure 1: Schematic diagram of the Ion Beam Sputtering system.

Table 2: The deposition conditions for titanium nitride thin films by Ion Beam Sputtering.

Deposition parameters specifications	
Target	Ti
Sputtering gas	Ar
Reactive gas	N ₂
(Ar:N ₂) gas ratio	7:7, 15:7, 30:7 and 50:7
Base pressure (Torr)	2.2×10 ⁻⁵
Working pressure (Torr)	5.5×10 ⁻³
Substrate temperature (°C)	400
Electron beam current (mA)	25
Acceleration Voltage (kV)	2.2
Deposition time (min)	60

Ar and N₂ ions were accelerated toward Ti target at fixed energy of 2.2 keV and the current of 25 mA/cm² throughout the experiments. The phase and crystalline structure of the samples were characterized by X-ray diffraction (XRD) using a Philips-PW 1800 with Cu K_α radiation (40 kV, 30 mA). The scan rate was 1°/min and 2θ angle range of 30 to 100° was selected. Surface topography was studied using scanning electron microscopy.

Electrochemical studies on samples were conducted using a computer-assisted potentiostat (273A, EG & G, USA). The test was carried out in 3.5 wt% (0.6 M) NaCl solution using conventional three electrode cell equipped with produced samples as working electrode (1 cm²), and platinum and calomel as counter and reference electrodes, respectively. The reference electrode was connected to a Luggin capillary and the tip of the Luggin capillary was kept closer to the surface of the working electrode to minimize IR drop. The sample was kept in NaCl solution for an hour in order to establish the open circuit potential (E_{OCP}). The change in open circuit potential (OCP) values were monitored and represented as potential vs. time plot. The potentiodynamic polarization (Tafel plots) has been represented as potential vs. log i. Corrosion current density (i_{corr}) was obtained from the intersection of extrapolation of cathodic and anodic Tafel slopes back to the corrosion potential (E_{corr}). The elemental analysis of the samples after corrosion test was

performed using energy dispersive spectroscopy (EDS) analysis.

3. Results and Discussion

3.1. XRD

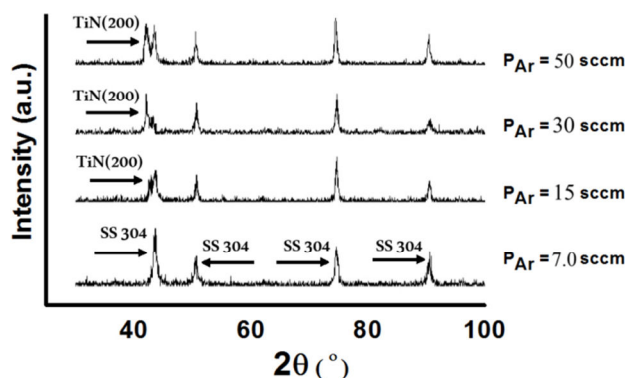
XRD patterns of deposited samples at different gas ratios (shown in Table 3) are illustrated in Figure 2. As is clear from Figure 2, TiN phase is not formed for S₁ and only austenite phase with sharp peaks corresponding to γ-Fe(111), γ-Fe(200), γ-Fe(220) and γ-Fe(311) at 2θ = 43.7°, 50.7°, 74.8° and 90.0°, respectively, is observed.

The TiN samples S₂ to S₄ in addition to four SS peaks showed one peak at 2θ = 42.611° corresponding to TiN(200) with a rock salt faced-centred cubic crystal structure (JCPDS Card No: 06-0642). The intensity of (200) peak increased by the flow rate of argon. It can be observed that at high Ar:N₂ flow ratio of 50:7 (sample S₄), maximum intensity is observed for (200) peak which revealed golden yellow color. This can be explained by the influence of deposition parameter. The crystallite size, D, is obtained using the Scherrer equation (Eq. 1)[11].

$$D = \frac{k\lambda}{B \cos \theta} \quad (1)$$

Table 3: Deposited samples under different Ar/N₂ flow ratios.

Sample	S1	S2	S3	S4
Ar/N ₂	7.7	15.7	30.7	50.7

**Figure 2:** XRD patterns of TiN deposited at various argon/nitrogen flow ratios of (a) 7, (b) 15, (c) 30 and (d) 50.

where, k is a dimensionless constant that is related to the shape and distribution of crystallites, λ is the wavelength of X-ray and θ is the Bragg angle. B is the full width at half maximum of the peak intensity (FWHM) in radian given by (Eq. 2):

$$B = \sqrt{W_0^2 - W_i^2} \quad (2)$$

where, W_0 and W_i are the FWHM of the sample and the stress-free sample (annealed powder sample), respectively.

The crystallite size calculated for TiN(200) peak is given in Table 4. It can be seen that the crystallite size of the titanium nitride phase increased with Ar gas flow.

3.2. Potentiodynamic Polarization

Figure 3 shows the potentiodynamic polarization curves

of the samples at room temperature in 3.5 wt.% NaCl aqueous solution. It is found that the corrosion protection of samples is improved remarkably due to the titanium nitride coatings. The values of corrosion potential E_{corr} and corrosion current density I_{corr} are listed in Table 4. It can be observed from Figure 3 that the E_{corr} and I_{corr} change with increasing of Ar flow, indicating an improvement of corrosion resistance with increasing the argon flow. So, the optimum corrosion protection is observed for sample coated at 50 sccm Ar flow. It can be seen from Figure 4 (i-v per temperature) that with increasing of Ar flow from 7 sccm to 15 sccm, the corrosion potential (E_{corr}) increases from -211.96 mV to -202.62 mV and the corrosion current density decreases from 4.47 $\mu\text{A}/\text{cm}^2$ to 0.28 $\mu\text{A}/\text{cm}^2$. Further increase of Ar flow results in a better corrosion protection behavior such that for the sample coated at 50 sccm Ar flow, corrosion potential has increased to -9.5 mV.

Table 4: The crystal size and corrosion parameters for TiN/SS 304 at different Ar flows.

Sample	Ar flow (sccm)	Crystallite size (nm)	Corrosion current density ($\mu\text{A cm}^{-2}$)	Corrosion potential (mV vs. SCE)
TiN/SS 304	7.0	---	4.47	-211.96
	15	32	0.28	-202.62
	30	49	0.11	-127.86
	50	53	0.06	-9.50

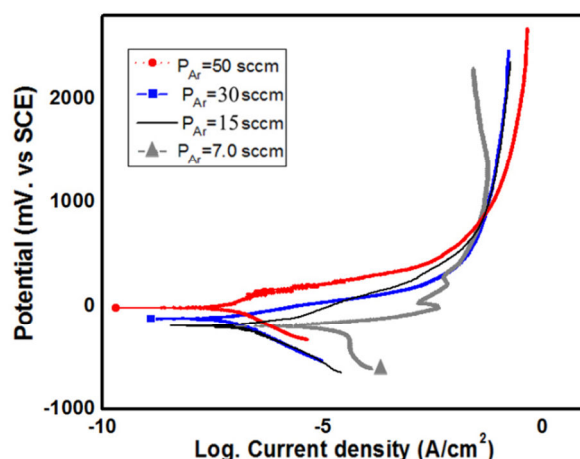


Figure 3: Polarization curves obtained for TiN coated samples at various argon/nitrogen flow ratios of 7, 15, 30 and 50.

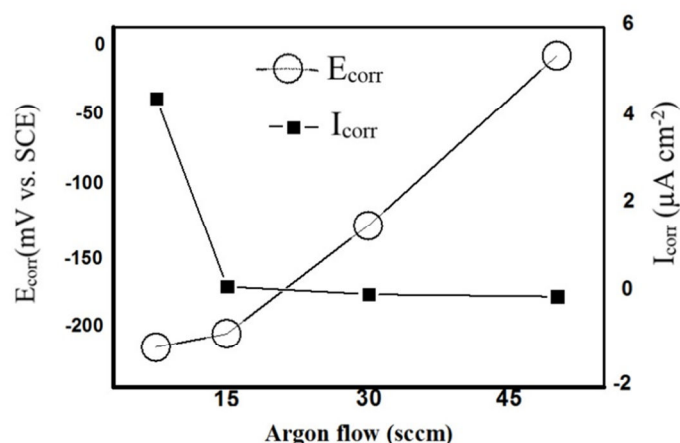


Figure 4: E_{corr} and I_{corr} for TiN coated samples at various argon/nitrogen flow ratios of 7, 15, 30 and 50.

3.3. SEM and EDS

SEM images of the samples taken after corrosion test are shown in Figure 5. According to this Figure, less surface damage is observed in sample coated with 50 SCCM flow. Prominent cracks can be seen in the SEM images of the samples (comparing Figures 5a and 5d), hence lower corrosion resistance of these samples (see Table 4) can be due to the formation of these cracks which provide extra effective surface for corrosion in the corroding media. These cracks are resulted from the initiation of pitting at locations prone to corrosion in the samples and their propagation through the grooves between the large grains. Quantitative view of EDS plots

in Figure 6 shows that the surfaces with good corrosion protection have higher amounts of Ti element which means that the corrosive solution couldn't penetrate into the steel. For Ar flow of 7 sccm, the EDS analysis show a great amount of Fe and Cr which confirms the demolition of TiN coating and the subsequent penetration of corrosive solution into the steel substrate. The sample deposited at 50 sccm Ar flow with the maximum corrosion potential and minimum corrosion current density has the best appearance and also the maximum amount of coated element in EDS plots. So, the TiN coating produced at 50 sccm Ar flow has increased the corrosion resistance of 304 stainless steel.

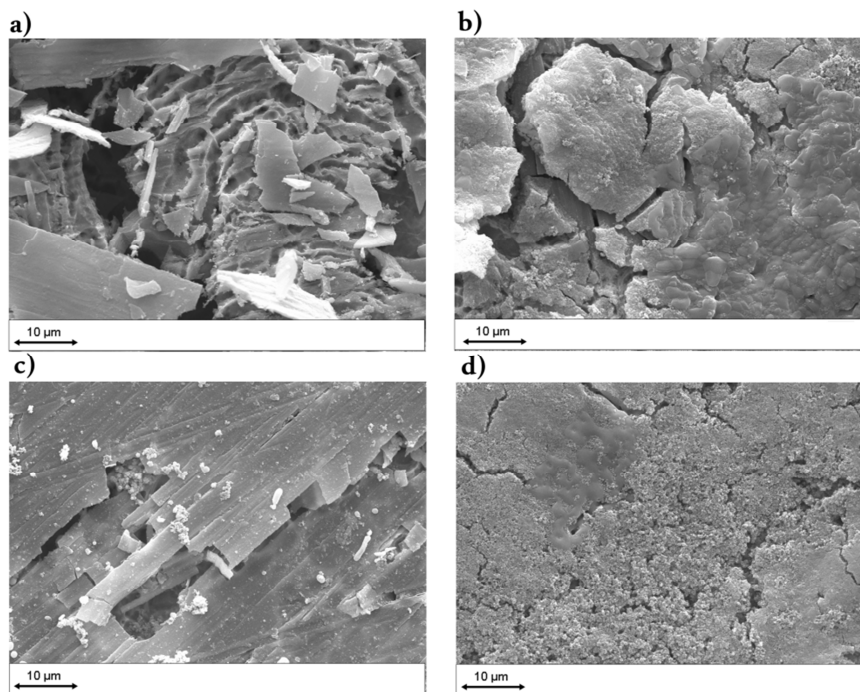


Figure 5: SEM images of TiN deposited at various argon/nitrogen flow ratios of (a) 7, (b) 15, (c) 30 and (d) 50.

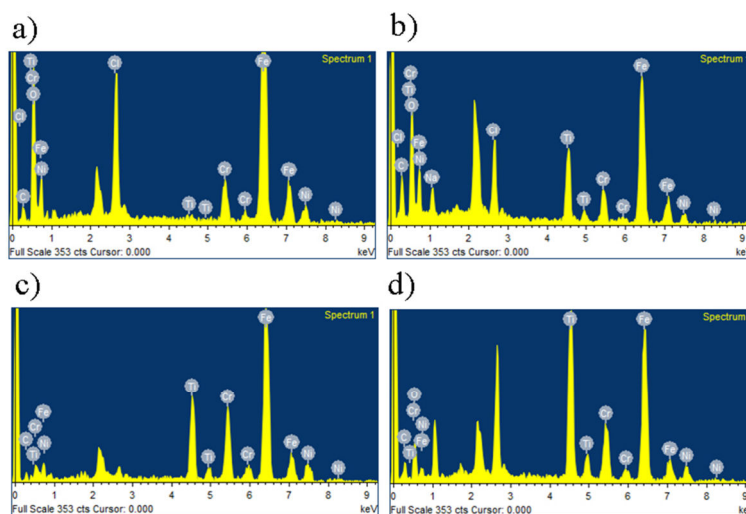


Figure 6: EDS images of TiN deposited at various argon/nitrogen flow ratios of (a) 7, (b) 15, (c) 30 and (d) 50.

4. Conclusion

Titanium nitride films were deposited on 304 stainless-steel substrates at a 400 °C and various nitrogen/argon flow ratios. The nano-structures of the films obtained from XRD analysis showed that films deposited at nitrogen/argon flow ratios from 15 to 50 sccm exhibited a TiN phase. But an increase of Ar concentration in TiN phases produces a high intensity of (200) peak. The

corrosion behavior of AISI 304 stainless steel was studied by deposition of TiN coatings at different gas ratios. Potentiodynamic polarization analysis performed in 3.5% NaCl solution showed that the highest corrosion protection was achieved for 50 sccm Ar flow. It was shown that there is an optimum Ar flow and the corrosion current density decreased by two orders of magnitude in comparison with the bare stainless steel.

5. References

1. I. Jauberteau, A. Bessaudou, R. Mayet, J. Cornette, J. Louis Jauberteau, P. Carles, T. Merle Méjean, Molybdenum Nitride Films: Crystal Structures, Synthesis, Mechanical, Electrical and Some Other Properties, *Coatings*, 5(2015), 656-687.
2. A. R. Grayeli Korpi, Kh. M. Bahmanpour, Effect of Nitriding Temperature on the Nanostructure and Corrosion Properties of Nickel Coated 304 Stainless Steel, *Prog. Color Colorants Coat.*, 10(2017), 85-92
3. B. Avasarala, P.Haldar, Electrochemical oxidation behavior of titanium nitride based electrocatalysts under PEM fuel cell conditions, *Electrochimica Acta*, 55(2010), 9024-9034.
4. S. Zhang, W. Zhu, TiN coating of tool steels: a review, *J. Mat. Process.Technol.*, 39(1993), 165-177
5. R. Buhl, H.K. Pulker, E. Moll, TiN coatings on steel, *Thin Solid Films*, 80(1981) 265-270.
6. S. M. Borah, H. Bailung, J. Chuti, Decorative Titanium Nitride Colored Coatings on Bell-Metal by Reactive Cylindrical Magnetron Sputtering, *Prog. Color Colorants Coat.* 3(2010),74-80
7. J. Yang, Y. Jiang, J. Hardell, B. Prakash, Q. Fang, Influence of service temperature on tribological characteristics of self-lubricant coatings: A review, *Front. Mater. Sci.*, 7(2013), 28-39.
8. Y. L. Jeyachandran, Sa.K. Narayandass, D. Mangalaraj, Sami Areva, J.A. Mielczarski, Properties of titanium nitride films prepared by direct current magnetron sputtering, *Mater. Sci. Eng. A.*, 445-446 (2007), 223-236
9. I. Kim, F. Khatkhatay, L. Jiao, G. Swadener, J. I. Cole, J. Gan, H. Wang, TiN-based coatings on fuel cladding tubes for advanced nuclear reactors, *J. Nuclear Mater.*, 429(2012), 143-148.
10. Y. Zhao, G. Lin, J. Xiao, W. Lang, C. Dong, J. Gong, C. Sun, Synthesis of titanium nitride thin films deposited by a new shielded arc ion plating, *Appl. Surf. Sci.*, 257(2011) 5694-5697.
11. V. Chawla, R. Jayaganthan, R. Chandra, Structural characterizations of magnetron sputtered nanocrystalline TiN thin films, *Mater. Character.*, 59(2008), 1015-1020.

How to cite this article:

A. R. Grayeli Korpi, P. Balashabadi, M. M. Larijani, M. Habibi, A. Hamidi, M. Malek, Effect of Gas Ratio on Tribological and Corrosion Properties of Ion Beam Sputter Deposited TiN Coatings. *Prog. Color Colorants Coat.*, 11 (2018), 129-135.

